Theoretical Study of in Elastic Properties of Fayalite (Fe_2SiO_4) at high temperature

DR. Pankaja Singh[1], Professor, Department of Physics, Govt. S.V. College Raisen
pankajasingh@gmail.com

Charu Dubey[2], Research Scholar, Department of Physics, MLBCollege Bhopal
charudubey06@gmail.com

Abstract

Fayalite is named for the Island of Fayal of the Azores. It is one of two minerals that are simply known as olivine. The other mineral is forsterite.Fayalite is the iron rich member with a pure formula of Fe_2SiO_4.Forsterite is the magnesium rich member with a pure formula of Mg_2SiO_4. The two minerals form a series where the iron and magnesium are substitutable for each other without much effect on the crystal structure. Fayalite due to its iron content has a higher index of refraction, is heavier and has a darker color than forsterite. Otherwise they are difficult to distinguish and virtually all specimens of the two minerals contain both iron and magnesium. For simplicity sake and general public recognition, they are often treated as one mineral, olivine. Olivine however is actually not officially recognized as a mineral. Olivine's gemstone variety is known as peridot. Most peridot is the magnesium rich forsterite, not fayalite. Fayalite's higher iron content makes for darker, less attractive specimens that are not generally used as gemstones.

The reported elastic properties of fayalite are limited to three dilatational wave velocities along the a, b and c axes of imperfect fayalite crystal, the ultrasonic velocities in polycrystalline sample; revised data of and the compressibility's determined by a volumetric technique, and an X-ray diffraction technique The elastic properties of other olivine type silicate minerals have never been reported.

The elastic constants were determined by an RPR method. The theory and the technical details of this method have been reported by OHNO (1976), SUMINO et al.

(1976), and the details of measuring the temperature variation of elastic constants have been described in SUMINO et al. (1977).

Key Words- Fe_2SiO_4, orthorhombic, Peridot, Elastic modulus

Introduction

Fayalite (Fe_2SiO_4; commonly abbreviated to Fa), also called iron chrysolite, is the iron-rich end-member of the olivine solid-solution series. In common with all minerals in the olivine group, fayalite crystallizes in the orthorhombic system (space groupPbnm) with cell parameters a 4.82 Å, b 10.48 Å and c Å 6.09. Iron rich olivine is a relatively common constituent of acidic and alkaline igneous rocks such as volcanic obsidians, rhyolites, trachytes and phonolites and plutonic quartz syenites where it is associated with amphiboles. Its main occurrence is in ultramaficvolcanic and plutonic rocks and less commonly in felsic plutonic rocks and rarely in granitepegmatite. It also occurs in lithophysae in obsidian. It also occurs in medium-grade thermally metamorphosed iron-rich sediments and in impure carbonate rocks. [1] Fayalite is stable with quartz at low pressures, whereas more magnesian olivine is not, because of the reaction olivine + quartz = orthopyroxene. Iron stabilizes the olivine + quartz pair. The pressure and compositional dependence of the reaction can be used to calculate constraints on pressures at which assemblages of olivine + quartz formed.

Fayalite can also react with oxygen to produce magnetite + quartz: the three minerals together make up the "FMQ" oxygen buffer. The reaction is used to control the fugacity of oxygen in laboratory experiments. It can also be used to calculate the fugacity of oxygen recorded by mineral assemblages in metamorphic and igneous processes.[2] Silicon (Si) is a common alloying element in advanced high strength steels, such as dual phase (DP) steel and transformation induced plasticity (TRIP) steel. However, the addition of Si often leads to red scale (mainly consisting of Fe_2O_3), a surface defect of hot rolled steels. Some research has investigated the formation of red scale, commonly regarded as directly related to the presence of Fe_2SiO_4–FeO eutectic, which is formed by the combination of SiO_2 and FeO. The theoretical eutectic temperature (melting point) of Fe_2SiO_4–FeO is recognized as 1173 °C. When the reheating temperature of slabs is above 1173 °C, the liquid Fe_2SiO_4–FeO penetrates into the external scale along the grain boundary of the scale and forms

a net-like distribution. If the subsequent descaling temperature is below 1173 °C, the liquid net-like Fe_2SiO_4 solidifies and firmly bonds the steel substrate and iron scale, making it difficult to completely remove the FeO layer during descaling. The remaining FeO scale is oxidized into red Fe_2O_3 (red scale defect) during the subsequent cooling and rolling processes.[3-4]

Due to the close relationship between red scale and Fe_2SiO_4–FeO, some studies on Fe_2SiO_4–FeO in Si-containing steels have been carried out. Yuan et al. reported that the net-like morphology of Fe_2SiO_4–FeO is not obvious when the Si content is low. Mouayd et al. and Suarez etal.found that the amount and penetrative depth of Fe_2SiO_4–FeO increases with the Si content. In addition,[5] reported that the morphology of Fe_2SiO_4–FeO is blocky when the reheating temperature is below 1173 °C, because solid Fe_2SiO_4–FeO cannot penetrate into the external scale. However, when the reheating temperature is above 1173°C, the morphology of Fe_2SiO_4–FeO is net-like. Net-like Fe_2SiO_4–FeO is well known to more easily lead to red scale compared with blocky Fe_2SiO_4–FeO.

In summary, red scale is mainly caused by net-like Fe_2SiO_4–FeO, and only liquid Fe_2SiO_4–FeO can form a net-like morphology. Thus, more attention should be given to the liquid Fe_2SiO_4–FeO. During the industrial reheating process, solid Fe_2SiO_4–FeO forms first before 1173 °C is reached and then melts into liquid at temperatures above 1173°C. Besides, new liquid Fe_2SiO_4–FeO is gradually formed by the combination of SiO_2 andFeO at temperatures above 1173°C. Therefore, liquid Fe_2SiO_4–FeO can be classified into two types when the reheating temperature is above 1173°C. One forms by the melting of pre-existing solid Fe_2SiO_4–FeO, which has already formed below 1173°C. The other appears above 1173 °C which is liquid once it forms.[5] The former is termed as type-1 liquid Fe_2SiO_4–FeO and the latter is termed as type-2 liquid Fe_2SiO_4–FeO. The biggest difference between two types of liquid Fe_2SiO_4–FeO is that type-1 liquid Fe_2SiO_4–FeO is solid before 1173°C is reached, whereas type-2 liquid Fe_2SiO_4–FeO is liquid from the time it forms. The distributions and morphologies of both types of liquid Fe_2SiO_4–FeO may be different. It is necessary to study the difference in their morphologies due to the close relationship between red scale and liquid Fe_2SiO_4–FeO. Thus far, research on this subject has been rarely reported. The name fayalite is derived from Faial (Fayal) Island in the Azores where it was first described in 1840.[2]

Table : Chemical formula of Fe_2SiO_4

Chemical Formula:	Fe_2SiO_4
Composition:	Molecular Weight = 203.78 gm Iron 54.81 % Fe 70.51 % FeO Silicon 13.78 % Si 29.49 % SiO_2 Oxygen 31.41 % O 100.00 % 100.00 % = TOTAL OXIDE
Empirical Formula:	$Fe^{2+}{}_2(SiO_4)$
nvironment:	Ultra mafic silica-poor igneous rocks.
IMA Status:	Valid Species (Pre-IMA) 1840
Locality:	Fayal Island, Azores Link to MinDat.org Location Data.
Name Origin:	Named for the locality
Name Pronunciation:	Fayalite
Synonym:	Hortonolite - Mn,Mg ICSD 26375 Knebelite(Mn) PDF 31-633

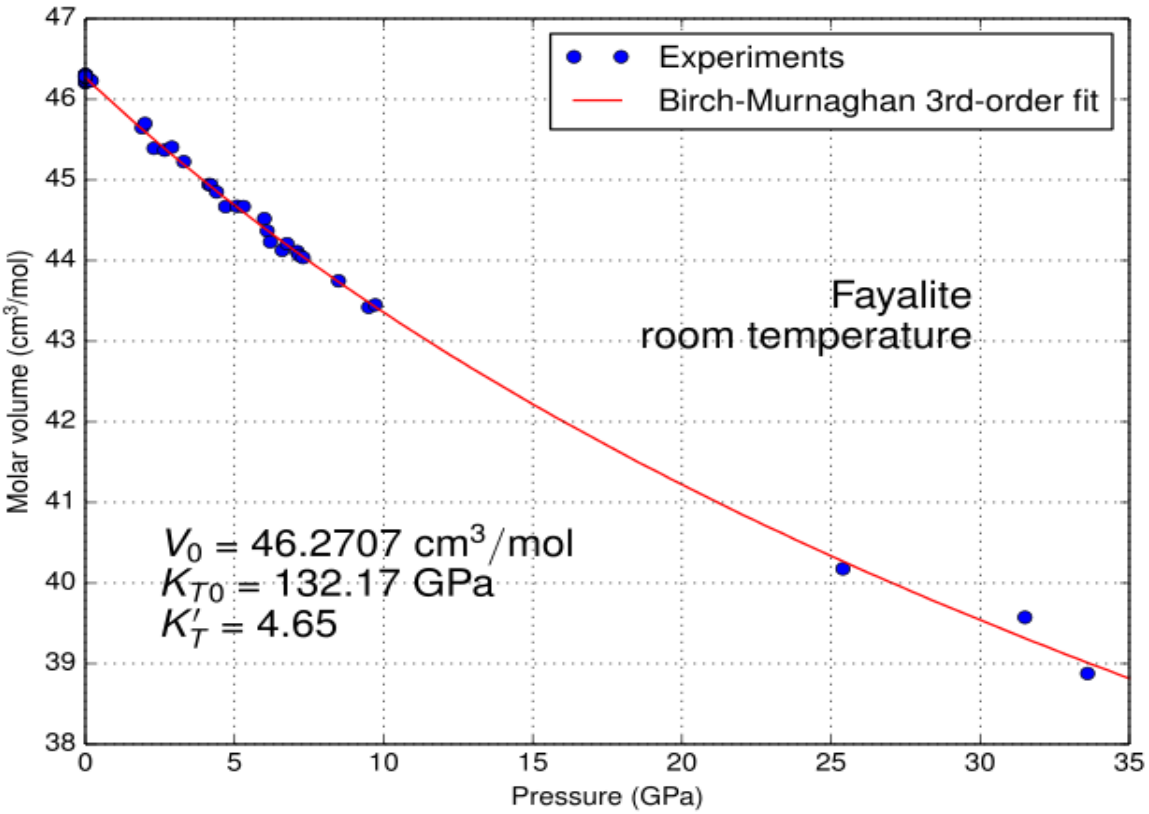

Figure :Molar volume vs. pressure at room temperature

Table :Elements detailed of Fe_2SiO_4

Symbol	Element	Atomic weight	Atoms	Mass percent

Fe	Iron	55.845	2	54.8110 %
Si	Silicon	28.0855	1	13.7827 %
O	Oxygen	15.9994	4	31.4063 %

Table : Mass composition by element (g/mol)FeSiO

General	
Category	Nesosilicate
Formula(repeating unit)	Fe_2SiO_4
Strunz classification	9.AC.05
Crystal system	Orthorhombic
Crystal class	Dipyramidal(mmm) H-M symbol: (2/m 2/m 2/m)
Space group	Pbnm
Unit cell	a = 4.8211, b = 10.4779 c = 6.0889 [Å]; Z = 4

Properties of Fe_2SiO_4

Color is yellowish green to greenish brown to black (lighter greens indicate a higher magnesium content and would be considered olivine or even forsterite).

Luster is vitreous; Transparency crystals are transparent to translucent; Crystal System is orthorhombic; 2/m 2/m 2/m; Crystal Habits include flatten tabular to box shaped crystals, but good crystals are rare. More commonly found as grains in alluvial gravels and as granular pockets in highly magnesium and iron rich volcanic rock. Also massive; Cleavage is distinct in two directions at 90 degrees;Fracture is conchoidal; Hardness is 6.5 – 7; Specific Gravity is approximately 4.3 (above average for non-metallic minerals) and the Streak is white.

Other Characteristics: Index of refraction is 1.87, moderate double refraction can usually be seen and crystals are typically striated.Associated Minerals are diopside, spinel, plagioclase feldspars, chromite, anorthite, biotite, cristobalite, hornblende, serpentine, obsidian, iron-nickel meteorites and augite. Notable Occurrences include the Salt Lake Crater, Oahu, Hawaii; Sugarloaf Mountain, Inyo County, California and Peridot, Gila County, Arizona, USA; Lipari Islands, Sicili and Mt. Vesuvius, Italy; France; Sweden and many other locations. Best Field Indicators are environment of formation, color, crystal habit, hardness and density. [5]

Table :PhysicalProperties of Fe_2SiO_4

Cleavage:	{010} Indistinct
Color:	Brown, Black, Black.
Density:	4.39
Diaphaneity:	Transparent to Translucent
Fracture:	Conchoidal - Fractures developed in brittle materials characterized by smoothly curving surfaces, (e.g. quartz).
Habit:	Granular - Generally occurs as anhedral to subhedral crystals in matrix.
Habit:	Massive - Granular - Common texture observed in granite and other igneous rock.
Hardness:	6.5 - Pyrite
Luminescence:	Non-fluorescent.
Luster:	Vitreous (Glassy)
Streak:	white
Gladstone-Dale:	CI meas= 0.055 (Good) - where the CI = (1-KPDmeas/KC) CI calc= 0.11 (Poor) - where the CI = (1-KPDcalc/KC) KPDcalc= 0.1726,KPDmeas= 0.1833,KC= 0.1939 Ncalc = 1.85 - 1.9
Optical Data:	Biaxial (-), a=1.731-1.824, b=1.76-1.864, g=1.773-1.875, bire=0.0420-0.0510, 2V (Calc) =54-66, 2V (Meas) =74-47. Dispersion weak, r > v.
Pleochroism (x):	greenish yellow, pale yellow, or pale amber.
Pleochroism (y):	orange yellow, orange yellow, or orange yellow.
Pleochroism (z):	greenish yellow, pale yellow, or pale amber.
Electron Density:	**Bulk Density (Electron Density)=4.22 gm/cc** note: Specific Gravity of Fayalite =4.39 gm/cc.
Fermion Index:	Fermion Index = 0.01 Boson Index = 0.99
Photoelectric:	**$PE_{Fayalite}$= 17.09** barns/electron **U=$PE_{Fayalite}$x □Electron Density= 72.16** barns/cc.
Radioactivity:	**GRapi = 0** (Gamma Ray American Petroleum Institute Units) Fayalite is **Not Radioactive**

The synthetic iron silicate fayalite («6-Fe2Si04) crystallizes with the same symmetry as the natural members of the olivine family. Despite extensive study of this mineral group, relatively little is known about its magnetic properties. The metal ions occupy two different octahedral positions in the structure, one, called Mj (4a),is located on a center of symmetry, the other one, M^j (4c), is situated on a mirror plane. The

compound undergoes an antiferromagnetic phase transition at Tc = 65.3(3) K to a colinear structure with spins parallel to the b-axis. An additional canting is observed below 23(3) K where Mx is canted without a resulting moment /I, 2/. A study of charge density by X-ray diffraction at 120K in this material is carried out in parallel to the polarized neutron work.

X ray diffraction and infrared spectroscopic measurements to pressures of 45–50 GPa, electrical resistivity and optical absorption to 70–80 GPa, and reflectance measurements to 225 GPa are presented for Fe_2SiO_4fayalite at 300 K. Diffraction results document that Fe_2SiO_4fayalite becomes amorphous on static loading to pressures in excess of 39 (±3) GPa, a pressure identical to that at which the "mixed phase" regime of fayalite commences under shock compression. As with more polymerized silicates, the high-pressure amorphization of metastable fayalite is associated with the SiO_4 tetrahedron becoming unstable relative to higher coordination of silicon. Infrared absorption spectroscopy reveals the pressure-induced change in coordination through a decline in intensity of the tetrahedral asymmetric stretching vibration, accompanied by an increase in amplitude at frequencies characteristic of SiO_6 vibrations. The coordination change is not quenchable to zero pressure, and infrared spectra of amorphous fayalite quenched from pressure document that the local structure of the sample is similar to that of crystalline Fe_2SiO_4. This represents the first example of the static synthesis of a glass without fusion in a silicate containing isolated tetrahedra. The electrical resistivity of initially crystalline Fe_2SiO_4 drops from approximately 2×10^5 ohm m at zero pressure to 10^{-3} ohm m at 79 GPa, with the pressure dependence of the resistivity decreasing at approximately the pressure of the coordination change (and amorphization). The electrical properties are quantitatively consistent with previous measurements, both under static and under shock wave loading. Optical transmission experiments demonstrate that in accord with the rapidly changing electron-transport properties of Fe_2SiO_4, a strong absorption edge decreases in energy from the ultraviolet to infrared energies of about 3500 cm^{-1} (0.4 eV) on compression to 70 GPa. However, the reflectance of Fe_2SiO_4 is less than 3.1% between 780 and 2100 nm at all pressures to 225 GPa, indicating that amorphous fayalite does not metallize to at least this pressure resistivity and optical results in terms of increased interactions between iron ions with increasing pressure in Fe_2SiO_4 and an approach toward a Fe^{3+}+Fe^{1+} metallic

configuration at high pressures. When combined with previous observations of amorphization at low temperatures and high pressures, our results suggest that transition to an amorphous phase is likely to be a general phenomenon in metastable silicates when the distortion of SiO_4tetrahedral becomes a major mechanism of compression.

Many of the uses of Mossbauer spectroscopy in solid- state chemistry are based on the analytical properties of this technique. Due to its sensitivity to hyperfine interactions (isomeric shift and quadruple interaction) the Mossbauer nuclei probe the ionic valence state, local bonding, and symmetry in a characteristic way. Consequently, Mossbauer spectroscopy has found wide application in the analysis of, e. g., iron-containing multiphase systems, notably when iron is present in different oxidation states, or experiences different local (electric or/and magnetic) interactions in the different phases. In homogeneous single-phase systems, typical analytical applications have been concerned with the determination of Fe2+JFe'+ ratios as well as with the distributions of the Mossbauer ions over non-equivalent sites of a given lattice structure.

Compositions

Fayalite (Fe_2SiO_4; commonly abbreviated to Fa), also called iron chrysolite, is the iron-rich end-member of the olivine solid-solution series. In common with all minerals in the olivine group, fayalite crystallizes in the orthorhombic system (space groupPbnm) with cell parameters a 4.82 Å, b 10.48 Å and c Å 6.09

Structure

Fe_2SiO_4 is an end member of Mg-rich $MgFe_2SiO_4$, which is believed to be a major mineral of the Earth's transition zone [6]. Since the presence of iron has a pronounced effect on elastic and thermodynamic properties of rock-forming minerals, having an impact on the geophysical processes in the Earth's interior, detailed characterization of Fe_2SiO_4 is of high interest. $Fe_2SiO_4$is known to exist in two phases: orthorhombic α fayalite and cubic γ spinel. The spinel phase was first synthesized in 1958 by Ringwood at 600 ◦ C and 3.8 GPa. It crystallizes in Fd 3¯m space group with Z = 8. Its natural occurrence was first reported much later in 2002 by Xie et al [4] in a

shock-induced melt vein in the Umbarger L6 chondrite. It is found to be stable in a wide range of high pressures and temperatures transforming directly from its orthorhombic phase at about 4 GPa and 1000^0C. Concerning the magnetic structure of Fe_2SiO_4 spinel, antiferromagnetic (AFM) ordering of the Fe spins was proposed at low temperatures T N ∼ 15 K on the basis of Mössbauerstudies[6]. Later, Choe et al measured in situ Mössbauer transmission spectra, which at room temperature and pressures up to 16 GPa showed a doublet characteristic of the paramagnetic (PM) state. In a more recent study, a PM–AFM transition was proposed to explain the λ -transition observed in the heat capacity spectrum of Fe_2SiO_4 -spinel at the temperature of 11.8 K. In our previous theoretical study the total focused on its electronic, magnetic and structural properties and lattice dynamics at p = 20 GPa and T = 0 showing that Fe_2SiO_4 spinel is an AFM Mott insulator. In this study, and examine the dynamic and thermodynamic properties of AFM Fe_2SiO_4 spinel in the pressure range up to 20 GPa using the density functional theory (DFT) approach. When compare them with those obtained for Mg_2SiO_4 spinel in order to understand the influence of cation exchange on lattice dynamics and thermodynamics in the ring woodite $(Fe,Mg)_2SiO_4$. The lattice dynamics and thermodynamic properties of the Mg_2SiO_4 spinel were the subject of several experimental and theoretical studies [7] in the past. In contrast, for its Fe-end counterpart, to the best of our knowledge, no theoretical study of the thermodynamic properties has been made previously. The paper is organized as follows. The methods of crystal optimization and phonon calculation are described, respectively. The phonon spectrum of Fe_2SiO_4 -spinel is analyzed and compared. The calculations were performed using the Vienna ab initio simulation package (VASP) based on the DFT approach employing the projector-augmented wave (PAW) method within the generalized gradient approximation (GGA) and periodic boundary conditions. In the case of Fe_2SiO_4 spinel, spin polarized DFT calculations were made. The wave functions were expanded in the plane waves up to the kinetic energy cutoff of 500 eV. The Monkhorst–Pack k -point generation scheme was used with a grid of 4 × 4 × 4 points in the irreducible part of the Brillouin zone. All calculations were performed in the 1 × 1 × 1 super cell containing 56 atoms: 8 Si, 16 Fe and 32 O. The model structure was fully (atomic and cell parameters) optimized at hydrostatic pressures equal to 12 .5,−10, −5, −2 . 5, 0, 5, 10 and 20 GPa. The electronic and ionic optimizations were continued until the energy differences between the successive electronic and ion cycles were less than 10−7 and 10−5 eV, respectively. For the

further phonon calculations, the forces on individual atoms had to be minimized. The force minimization process was stopped when all the forces on the individual atoms were lower than $10-5$ eV $A^{\circ}-1$. The maximum obtained force on an atom was $7 \times 10-6$ eV $A^{\circ}-1$. The calculations of the phonon properties were performed with the direct method as implemented in the PHONON program. To form the dynamical matrix, it uses the Hellmann–Feynman (HF) forces generated by displacing individual atoms from their ground-state positions. The HF forces were obtained in a set of single-point calculations using the DFT approach described in the previous section. In each single-point calculation, the HF forces are calculated on all atoms in the super cell after displacing one of the atoms in one crystallographic direction. The super cell symmetry and the site symmetry of non-equivalent atomic positions usually considerably reduce the number of necessary displacements. In the case of the spinel with a cubic $Fd\bar{3}m$ symmetry, there are three independent displacements, one for each non-equivalent atom (Fe, Si, and O). However, this scheme can be further complicated when introducing non-zero magnetic moments as is the case of Fe_2SiO_4 -spinel. In the AFM arrangement (figure 1), magnetic moments are aligned parallel in the diagonal Fe chains, and have opposite directions in successive (001) planes. Such AFM order causes lowering of the crystal symmetry down to the tetragonal I 4 1 / amd one with a = b = c and thus increases the number of necessary displacements to eight (Si along x and z , Fe and O along all three crystallographic directions). Thus the HF forces were generated for all 56 atoms in the super cell using three and eight displacements for Fe2 SiO 4 -spinel, respectively. The displacement step was equal to 0.02 $A.^{\circ}$ The lattice dynamics was then calculated within the cubic model in the PHONON program for both structures. In the case of AFM Fe 2 SiO 4 structure such an approximation was possible, because the tetragonal distortion was found to be very small and decreasing with increasing pressure (0.8–0.04% within -12 . 5–20 GPa). The ferromagnetic configuration in Fe_2SiO_4 has not been considered here since, as per discussion in, it leads to dynamically unstable crystal structure. The local Hubbard interaction U between the d electrons of the Fe ions has some impact on the lattice dynamics [7]. Besides the longitudinal–transverse optical (LO–TO) splitting induced by the insulating state, found an energy increase in the iron partial DOS. The largest changes were observed for the lowest phonon modes in the energy range between 10–20 meV. This energy shift is induced by the weaker screening of the interatomic forces in the Mott insulator, which leads to larger force constants and higher phonon

frequencies. Since the thermodynamic functions are not expected to be strongly modified by these changes, and because electronic convergence for certain atomic displacements could not be reached within the GGA + U scheme for negative pressures and do not take into account the Hubbard interaction in the present studies. Concerning the Fd3m symmetry, the phonon spectrum of X_2SiO_4 -spinel (X=Fe,Mg) consists of 42 dispersion curves. A group theory analysis shows that the 39 optical modes form the following irreducible representations at the Brillouin zone center: op = A 1g + 2A 2u + 2E u + E g + 4T 1u + 2T 2u + T 1g + 3T 2g where the A 1g , E g and T 2g modes are Raman active, the T 1u modes are infrared active and the A 2u , E u T 2u and T 1g are silent (inactive). All E modes are doubly degenerated and all T modes are triply degenerated.[7]

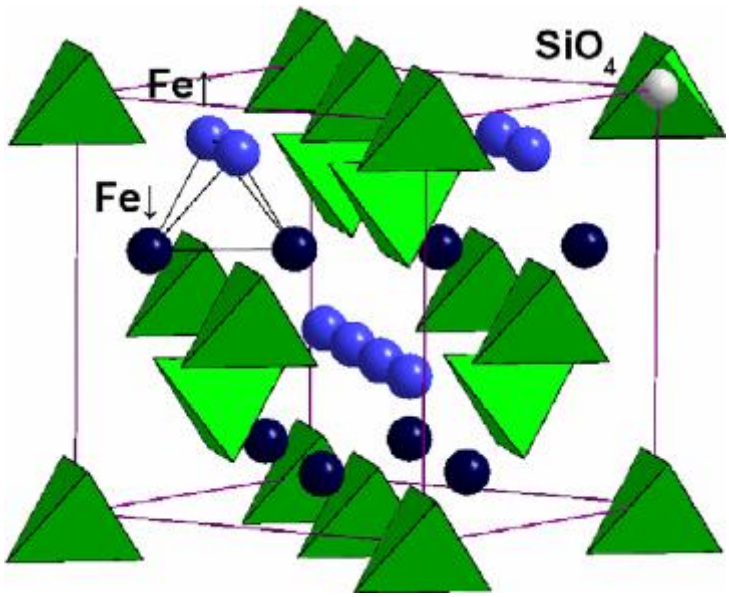

Figure :Structure of Fe_2SiO_4

A structural change in Fe_2SiO_4 spinel (ringwoodite) has been found by synchrotron powder diffraction study and the structure of a new high-pressure phase was determined by Monte-Carlo simulation method and Rietveld profile fitting of X-ray diffraction data up to 64 GPa at ambient temperature. A transition from the cubic spinel structure to a body centered orthorhombic phase (I-Fe_2SiO_4) with space group Imma and Z = 4 was observed at approximately 34 GPa. The structure of I-Fe_2SiO_4 has two crystallographically independent FeO_6octahedra. Iron resides in two different sites of six fold coordination: Fe1 and Fe2, which are arranged in layers parallel to (101) and (011) and are very similar to the layers of FeO_6octahedra in the spinel

structure. Silicon is located in the six fold coordination in I-Fe_2SiO_4. The transformation to the new high-pressure phase is reversible under decompression at ambient temperature. A martensitic transformation of each slab of the spinel structure with translation vector <1/8→1/8→1/8→> generates the I-Fe_2SiO_4 structure. Laser heating of I-Fe_2SiO_4 at 1500 K results in a decomposition of the material to rhombohedralFeO and SiO_2stishovite.[7]

FeKβ X-ray emission measurements at high pressure up to 65 GPa show that the transition from a high spin (HS) to an intermediate spin (IS) state begins at 17 GPa in the spinel phase. The IS electron spin state is gradually enhanced with pressure. The Fe^{2+} ion at the octahedral site changes the ion radius under compression at the low spin, which results in the changes of the lattice parameter and the deformation of the octahedra of the spinel structure. The compression curve of the lattice parameter of the spinel is discontinuous at ~20 GPa. The spin transition induces an isostructural change.

Elastic Properties of Fe_2SiO_4

The reported elastic properties of fayalite are limited to three dilatational wave velocities along the a, b and c axes of imperfect fayalite crystal, the ultrasonic velocities in polycrystalline sample; revised data of and the compressibility's determined by a volumetric technique, and an X-ray diffraction technique The elastic properties of other olivine type silicate minerals have never been reported.

The elastic constants were determined by an RPR method. The theory and the technical details of this method have been reported by OHNO (1976), SUMINO et al. (1976), and the details of measuring the temperature variation of elastic constants have been described in SUMINO et al. (1977). Measurement of resonance frequencies was made at temperatures between room temperature and 410°C on the lower ca. 30 vibrational modes for each specimen as listed in the modes follows those of OHNO (1976), and the observed values (Fobs) of resonance frequencies, the calculated most probable values (Fcal), and the normalized residuals [ΔF=(Fobs-Fcal)/Fobs] are presented. At high temperatures up to 410°C, the resonance frequencies were measured at irregular temperature intervals. [18]

Fe2SiO4 olivine Measurement of resonance frequencies was made at room temperature on the lower 30 vibrational modes for two specimens Fe2SiO4 (TA) and

Fe2SiO4 (TB). The higher temperature measurement up to 410°C was made on the lower 28 vibrational modes for Fe2SiO4 (TA) only. The relative deviations O-C are almost within 0.2% over the whole range of temperature. Results of elastic constants determinations and their temperature derivation.

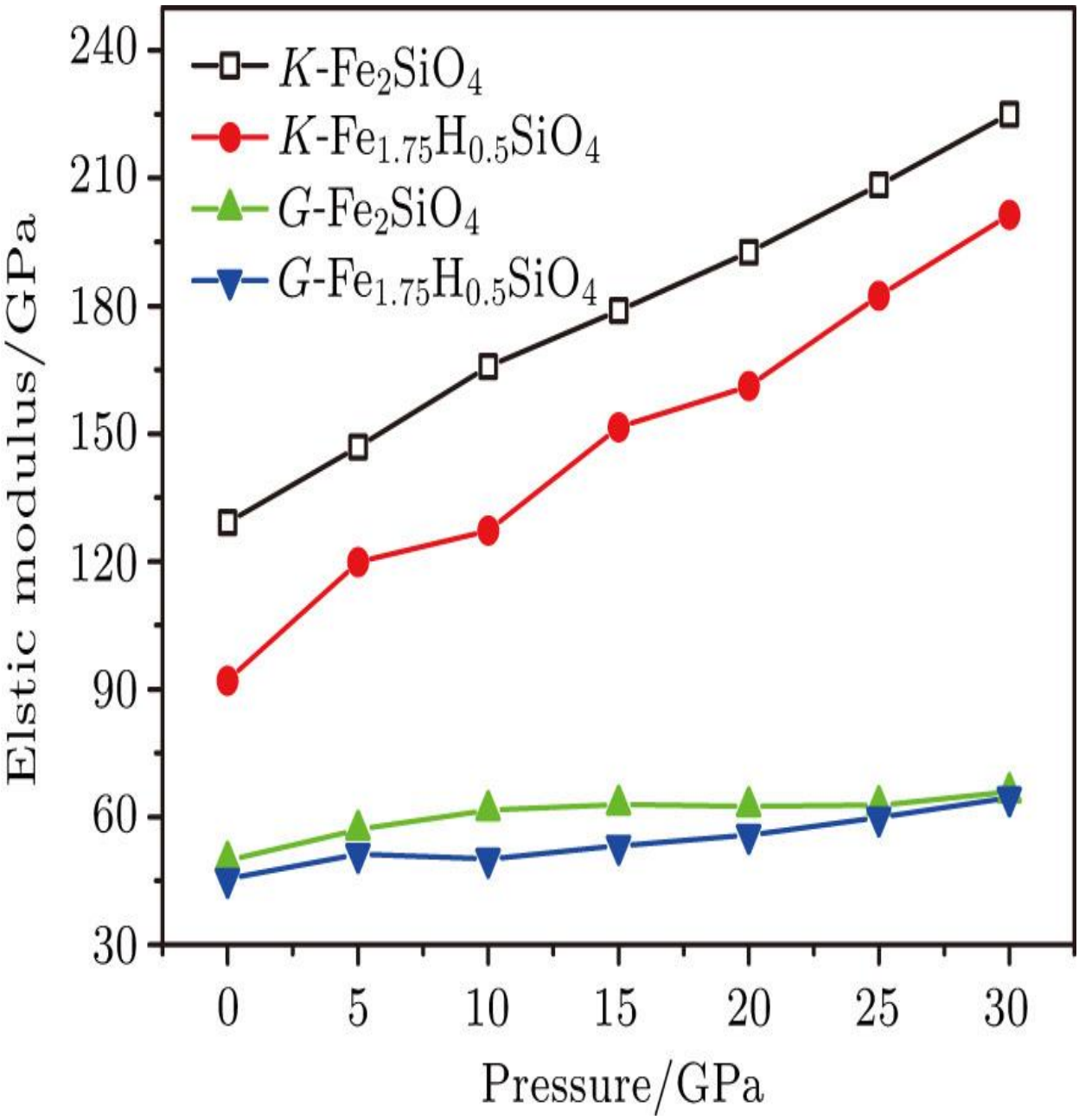

Figure :Elastic Property of Fe2SiO4 under pressure

Temperature Variation

Thermal expansion of single-crystal fayalite has been measured by a dilatometric method at temperatures between 25 °C and 850 °C. The results show the presence of anomalous expansion in the *b* axis, which is correlated to the anomalous variation of

elastic moduli with temperature. Grüneisen's parameter is 1.10 and the thermal Debye temperature is 565 K, which is close to the acoustic Debye temperature of 511 K.

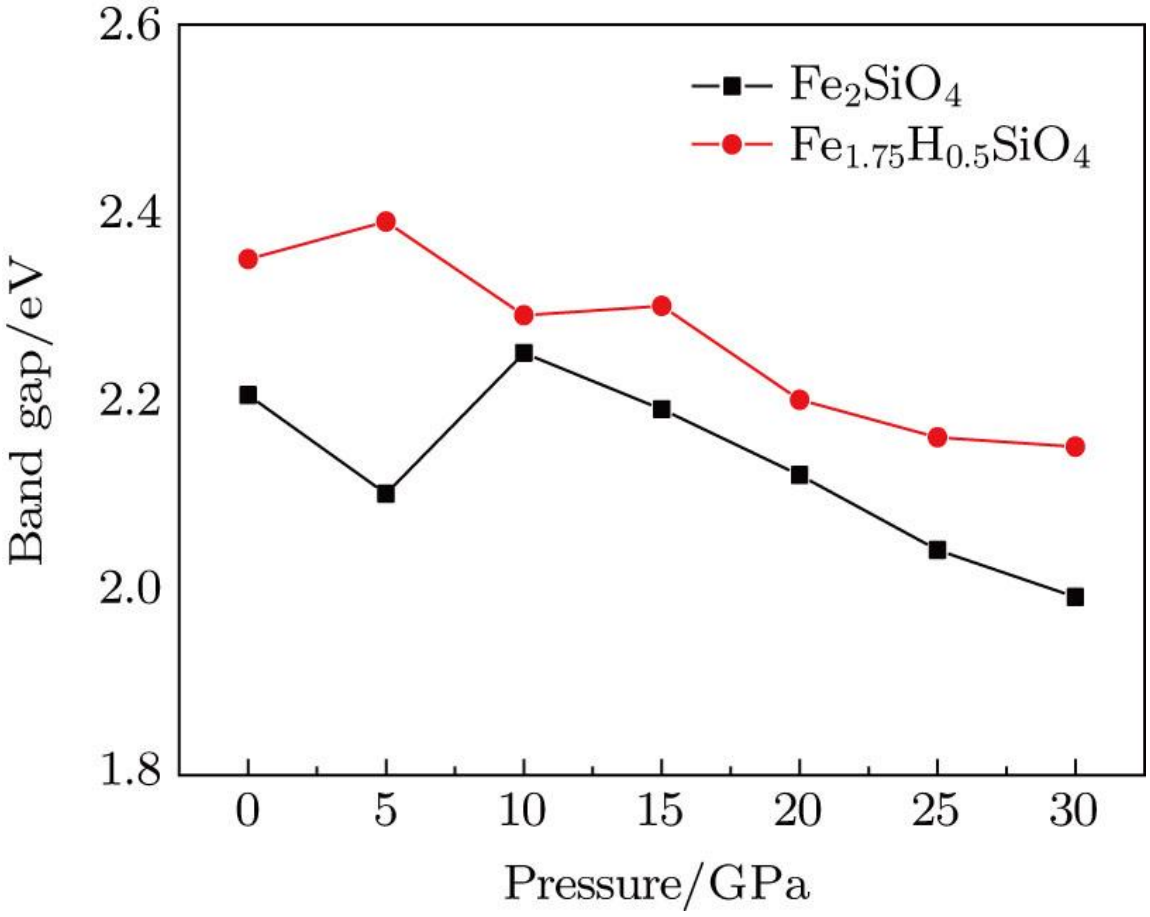

Figure :Temperature pressure under band gap of Fe_2SiO_4

Measurements of equation of state parameters for minerals of the mantle's transition zone at relevant high pressures and temperatures provide the key to interpreting seismic observations in terms of composition and temperature. Seismic tomography studies have parameterized lateral variations in travel time with variations in iron content, silica content, and temperature. [20] However these studies have been limited in part by the lack of tightly constrained equation of state parameters for relevant minerals and conditions. Ringwoodite $(Mg,Fe)_2SiO_4$ is the spinel-structured polymorph of olivine and likely the predominant mineral in the deep part of the transition zone While many measurements exist for the high pressure, high temperature equation of state at transition zone conditions at and close to the Mg end-member, only a small suite of measurements exist for Fe-ringwoodite and none of these are at the pressures and temperatures of the transition zone. Significant

uncertainties are introduced by extrapolating these results to relevant high pressures and temperatures, and therefore the effect of iron on the density and bulk modulus of ringwoodite is not well-constrained at the conditions of the transition zone. Our approach is to measure the density of Fe end-member ringwoodite using synchrotron X-ray diffraction techniques combined with laser heating in the diamond anvil cell. Together with previous measurements across the ringwoodite compositional range, our new equation of state allows interpretation of the seismic observations, both global and local, in terms of iron content and temperature. When measured the density of iron-ringwoodite and its pressure and temperature dependence at conditions of the mantle transition zone using the laser-heated diamond anvil cell in conjunction with X-ray diffraction.[20] New data combined with previous measurements constrain the thermoelastic properties of ringwoodite as a function of pressure and temperature throughout the transition zone. Our best fit Mie-Grüneisen-Debye equation of state parameters for Fe end-member ring woodite are V_0 = 42.03 cm_3/mol, K_0 = 202 (4) GPa, $K' = 4$, γ_0 = 1.08 (6), q = 2, and θ_D = 685 K. This new equation of state revises calculated densities of the Fe end-member at transition zone conditions upwards by ∼0.6% compared with previous formulations. Combine our data with equation of state parameters across the Mg-Fe compositional range to quantify the effect of iron and temperature on the density and bulk sound velocity of ringwoodite at pressure and temperature conditions of the Earth's transition zone. The results show that variations in iron content and temperature have opposing effects on density and bulk sound velocity, suggesting that compositional (iron content) and temperature variations in the transition zone may be distinguished using seismic observables.The elongation of the specimens Al i (~ l i - l i ~ ; h length of specimen, i: three crystallographic orientations, r: at reference temperature) recorded on a strip chart were read at temperature intervals, A T, of 25 K and relative expansion Yi(T)=A lfl~ r are listed in Table 1. Relative expansions in the a and b axes are almost the same and that in the c axis is somewhat larger. It is noted that the expansion in each orientation is reversible for heating and cooling runs. Linear and volume expansion coefficients are calculated by **1** AY~ I+Y i AT.

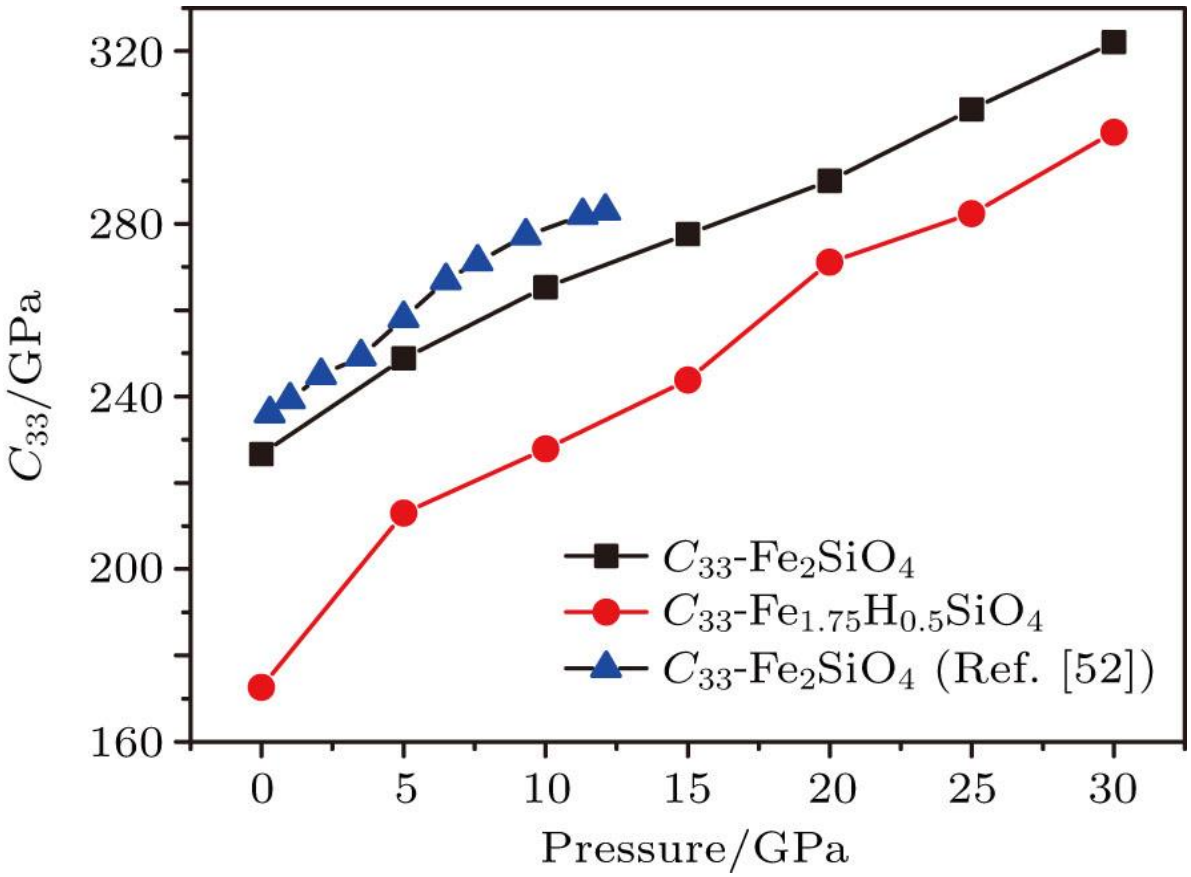

Figure :Temperature pressure under C_{33}/ GPa of Fe2SiO4

Energy-dispersive x-ray diffraction spectra for γ-Fe_2SiO_4 (spinel) collected in situ at 400° C and pressures to 24 GPa constitute the basis for an elevated-temperature static compression isotherm for this important high-pressure phase. A Murnaghan regression of these molar volume measurements yields 177.3 (±17.4) GPa and 5.4(±2.5) for the 400° C, room pressure values of the isothermal bulk modulus ($K_{P\,0}$) and its first pressure derivative ($K'_{P\,0}$), respectively. When compared to the room-T determinations of $K_{P\,0}$ available in the literature, our 400° C $K_{P\,0}$ yields -4.1 (±6.2)×10^{-2}GPa/degree for the average value of $(\partial K/\partial T)_{P\,0}$ over the temperature interval 25° C<T<400° C.[21]

A five-parameter $V(P,T)$ equation for γ-Fe_2SiO_4 based on simultaneous regression of our data combined with the elevated P-Tdata of Yagi et al. (1987) and the extrapolated thermal expansion values from Suzuki et al. (1979) yields isochores which have very little curvature [$(\partial^2T/\partial P^2)_v \cong 0$], in marked contrast to the isochores for fayalite (Plymate and Stout 1990) which exhibit pronounced negative curvature [$(\partial T/\partial P^2)_v<0$]. Along the fayalite/$\gamma$-$Fe_2SiO_4$ reaction boundary ΔV_R varies from a minimum of approximately 8.3% at approximately 450° C to approximately 8.9% at 1200° C. Extrapolation of the fayalite and γ-Fe_2SiO_4 V (P, T) relationships to the

temperature and pressure of the 400 km discontinuity suggests a ΔV_R of approximately 8.4% at that depth, approximately 10% less than the 9.3% ΔV_R at ambient conditions.[21]

Uses of Fe_2SiO_4

A worldwide search is on for cheap processes to sequester CO_2 by mineral reactions, called enhanced weathering. Removal by reactions with olivine is an attractive option, because it is widely available and reacts easily with the (acid) CO_2 from the atmosphere. When olivine is crushed, it weathers completely within a few years, depending on the grain size. All the CO_2 that is produced by burning one liter of oil can be sequestered by less than one liter of olivine. The reaction is exothermic but slow. To recover the heat produced by the reaction to produce electricity, a large volume of olivine must be thermally well-isolated. The end-products of the reaction are silicon dioxide, magnesium carbonate, and small amounts of iron oxide.[22-23] Olivine is a used as a substitute for dolomite in steel works. Olivine is also used to tap blast furnaces in the steel industry, acting as a plug, removed in each steel run.

The aluminium foundry industry uses olivine sand to cast objects in aluminum. Olivine sand requires less water than silica sands while still holding the mold together during handling and pouring of the metal. Less water means less gas (steam) to vent from the mold as metal is poured into the mold. In Finland, olivine is marketed as an ideal rock for sauna stoves because of its comparatively high density and resistance to weathering under repeated heating and cooling.[24]

Conclusion

Liquid Fe_2SiO_4–FeO is classified into two types. The present study investigates the difference in morphology between these two types of liquid Fe_2SiO_4–FeO. The results show that, compared with type-2 liquid Fe_2SiO_4–FeO, type-1 liquid Fe_2SiO_4–FeO is more likely to form a net-like morphology. The penetration depth of type-1 liquid Fe_2SiO_4–FeO is also larger at the same oxidation degree. Red scale defect is known to be caused by the net-like Fe_2SiO_4–FeO. Therefore, type-1 liquid Fe_2SiO_4–FeO should be avoided in order to eliminate red scale defect. Net-like Fe_2SiO_4–FeO may be alleviated by two methods: decreasing the oxygen concentration in the heating furnace and increasing the reheating rate before the melting point of Fe_2SiO_4–FeO is

reached. In addition, FeO is distributed with a punctiform or lamellar morphology on Fe_2SiO_4.

References

1. D. C. Presnall (1995), ed. by T. J. Ahrens, AGU vol. 2, American Geophysical Union, Washington, D.C., pp. 248–268
2. Deer, W. A., Howie, R. A., and Zussman, J. (1992). Harlow: Longman
3. Mingxing Zhou, GuangXu *, Haijiang Hu, Qing Yuan and JunyuTianMetals**2017**, 7(1), 8
4. Okada, H.; Fukagawa, T.; Ishihara, H. Prevention of red scale formation during hot rolling of steels. ISIJ Int.**1995**, 35, 886–891
5. He, B.; Xu, G.; Zhou, M.X.; Yuan, Q. Metals**2016**, 6, 137–145.
6. M MSinha and HarleenKaur Journal of Physics: Conference Series 759 2016.
7. Mariana Derzsi Journal of Physics Condensed Matter 23(10):105401
8. Yuan, Q.; Xu, G.; Zhou, M.X.; He, B..Metals**2016**, 6, 94–103.
9. Yuan, Q.; Xu, G.; Zhou, M.X.; He, B..Int. J. Min. Met. Mater.**2016**, 23, 1–8.
10. Garnaud, G.; Rapp, R.A. Oxid. Met.**1977**, 11, 193–198.
11. Staettle, R.W.; Fontana, M.G. Springer: New York, NY, USA, 1974; pp. 239–356
12. Abuluwefa, H.; Guthrie, R.I.L.; Ajersch, F. Oxid. Met.**1996**, 46, 423–440.
13. Chen, R.Y.; Yuen, W.Y.D. Oxid. Met.**2003**, 59, 433–468.
14. Serpentine, American Heritage Dictionary
15. *Rudler, Frederick William (1911).. In Chisholm, Hugh.* ***24*** *(11th ed.). Cambridge University Press. pp. 675–677.*
16. *Www.minerals.net*. Retrieved 4, 2018.
17. Norman H. Sleep, Dennis K. Bird, Emily C. Pope. hil. Trans. R. Soc. B 2011 366, 2857–2869
18. Yoshio Sumino J. Phys. Earth, 27, 209-238, 1979
19. Ohno I (1976). J Phys Earth 24: 355–379
20. Matthew Armentrout and Abby Kavner. Geophysical research letters, 38, L08309,2011
21. Isao Suzuki*, Kiyoshi Seya, Humihiko Takei 1, and Yoshio Sumino PhysChem Minerals (1981) 7:60-63
22. *Goldberg, P.; Chen, Z.-Y.; O'Connor, W.; Walters, R.; Ziock, H. 2000. Technology.* ***1*** *(1): 1–10.*
23. *Schuiling, R. D.; Krijgsman, P. 2006. Climatic Change.* ***74*** *(1–3): 349–54.*

24. *Ammen, C. W. 1980. The Metal Caster's Bible. Blue Ridge Summit PA: TAB. p. 331.*